^{6}He neutron distribution radius from ^{7}Li$(p,2p)^6$He reaction

V. B. Shostak,[1] G. P. Palkin,[1] N. I. Woloshin,[1] V. P. Likhachev,[2] M. N. Martins,[2] and M. T. F. da Cruz[2]
[1]*Institute for Nuclear Research, Kiev, Ukraine*
[2]*Laboratório do Acelerador Linear, Instituto de Física, Universidade de São Paulo, Caixa Postal 66318, 05315-970 São Paulo, SP, Brazil*
(Received 21 June 2000; published 8 December 2000)

Differential cross sections for the reaction ^{7}Li$(p,2p)^6$He, at incident proton energy of 70 MeV, were analyzed in the framework of the DWTA approach. The point-nucleon root-mean-square radius for the neutron distribution of ^{6}He was deduced to be 2.85(7) fm.

DOI: 10.1103/PhysRevC.63.017602 PACS number(s): 21.10.Gv, 25.40.Ep, 27.20.+n

A great interest in the properties of β-unstable neutron-rich nuclei has recently arisen due to experiments using high-energy radioactive nuclear beams. Information on the dimensions of unstable nuclei has been extracted from interaction cross section measurements at high energies [1,2], and from the elastic scattering of protons on helium isotopes [3]. All these analyses used the Glauber theory in the so-called optical limit approximation (OLA). The available experimental and theoretical information concerning the root-mean-square (rms) radii of neutron and nuclear matter distributions for ^{6}He are summarized in Table I.

The high accuracy achieved in the determination of $R^n_{^6\mathrm{He}}$ (1%) shows discrepancies among the available information. In this situation it is interesting to use different experimental methods to measure $R^n_{^6\mathrm{He}}$ and also try an analysis not based on Glauber theory, which is a common feature of the available results.

The present work is an endeavor to extract $R^n_{^6\mathrm{He}}$ from the analysis of the low-energy quasifree knockout reaction ^{7}Li$(p,2p)^6$He. This approach was used in [11] to deduce the neutron and nuclear matter rms radii of ^{8}Be.

The procedure for the deduction of the rms nuclear radius from the low-energy knockout reaction cross sections is based on the analysis in the distorted-wave approximation for nonlocal realistic *t*-matrix (DWTA). This method was developed in [12,13] and then improved in [14–16] for the case of arbitrary geometry, eliminating ambiguities in the parameters and including indirect processes.

The model distorted wave functions (DWF) for entrance $(+)$ and exit $(-)$ channels, used in these calculations, incorporate refraction, absorption, and focusing [16]:

$$\Psi^{(+)}_{\vec{k}}(\vec{r}) = e^{-\gamma \vec{k} R_N} e^{i(\beta + i\gamma)\vec{k}\cdot\vec{r}} [1 + F e^{(\vec{r} - R\hat{k})^2/S^2}],$$
$$\Psi^{(-)}_{\vec{k}}(\vec{r}) = [\Psi^{(+)}_{-\vec{k}}(\vec{r})]^*, \tag{1}$$

where $\beta + i\gamma = D$ is the complex refractive index of the optical model. The quantity βk plays the role of a modified wave number and γ determines the damping. F, R, and S are the focusing parameters, and R_N is a normalization parameter, which normalizes the model distorted wave to a plane wave at a distance R_N, and can be chosen as the mass radius of the nucleus.

It was shown [11,14,16,17] that the DWTA calculations quantitatively reproduce the experimental cross sections, including off-shell and final state interaction (FSI) contributions, without free parameters, using for the parametrization of the off-shell *t* matrix and distorted model wave functions the experimental data for the cross sections of the involved processes.

The first study of ^{7}Li(p,pn) and ^{7}Li$(p,2p)$ reactions was reported in [17]. Results of the simultaneous measurement of the differential cross sections for both reactions at incident proton energy of 70 MeV were presented together with a DWTA analysis for the ^{7}Li$(p,pn)^6$Li reaction. These calculations were fulfilled on a realistic base using the full set of required cross sections and quantitatively reproduced the experimental data for both $1p$ and $1s$ shells of ^{7}Li.

For the reaction ^{7}Li$(p,2p)^6$He it is impossible to carry out the DWTA calculations with the same standard calculation scheme used in the cases of ^{4}He$(p,pn)^3$He, ^{4}He$(p,2p)^3$H [16], and ^{7}Li$(p,pn)^6$Li [17], since there are no data for the elastic and total cross sections of the reaction $(p,^6\mathrm{He})$.

A similar situation was resolved in our earlier work [11] using, to determine the DWF parameters, the cross sections for a hypothetical residual nucleus (a neighboring stable isotope, for which data exist) and fitting the focusing parameter *R*, which is proportional to the rms radius of the final nucleus [12,18]. Using this procedure it was possible to deduce the rms radius of ^{8}Be. The results presented in Ref. [11] show that the DWTA cross sections are strongly sensitive to *R*, and also that a change in *R* affects differently the cross sections at different energies or for different shells. So, by fitting only a single parameter, *R*, it was possible to generate DWTA cross sections that agree well with all groups of experimental data. This means that the change of *R* adequately accounts for the differences in FSI between neighboring isotopes. The pairs ^{8}Be-^{9}Be and ^{4}He-^{6}He are very similar: The extra neutron(s) has a small separation energy, causes practically no change to the charge radius, but increases the neutron radius [3,11].

According to this calculation scheme, as a first step, the ^{7}Li$(p,2p)^6$He differential cross sections are calculated in-

TABLE I. Theoretical and experimentally deduced nuclear matter ($R^m_{^6\mathrm{He}}$) and neutron ($R^n_{^6\mathrm{He}}$) rms radii of ^{6}He, assuming point-nucleon distributions.

Ref.	[2]	[3]	[4]	[5]	[6]	[7]	[8]	[9]	[10]
$R^m_{^6\mathrm{He}}$	2.48(3)[a]	2.30(7)[a]	2.33(4)[a]	2.50[a]	2.71(4)[a]	2.57(10)[a]	2.46[b]	2.40[b]	2.51[b]
$R^n_{^6\mathrm{He}}$	2.61(3)[a]	2.48(11)[a]	2.59(4)[a]				2.67[b]	2.65[b]	2.78[b]

[a]Values deduced from experimental data.
[b]Theoretical results.

cluding the interaction effects of the outgoing nucleons with the hypothetical residual nucleus in the final state (FSI effects), using the cross section of ^{4}He instead of ^{6}He.

The DWF parameters for this hypothetical final state (^{4}He) were unambiguously chosen from the requirement of: (1) a quantitatively correct description of the experimental data for the elastic (differential and integrated) and total cross sections for the interaction of the proton with ^{4}He in the exit channels [19–22]; and (2) agreement between the DWF and the exact wave function, obtained by numerical integration of the Schrödinger equation in a range comparable with the size of the nucleus. The procedure for the choice of parameters, an analysis of their ambiguity, and the calculation of the cross sections with the model wave functions, Eq. (1), are described in detail in Ref. [16]. The parameters of the distorted wave function for the exit channel were obtained for four different energies of the secondary proton [17]: 14, 22, 31, and 40 MeV (see Table II). For the DWF in the entrance channel the parameters from Ref. [17] were used.

Figures 1 and 2 show the differential cross sections for the ^{7}Li$(p,2p)^6$He reaction [17], for the $1s$ and $1p$ shells, used in the analysis, versus the energy of the secondary protons E_p. Also shown, as dashed curves, are the results of DWTA calculations for the hypothetical final state with DWF parameters taken from Table II. The calculations strongly overestimate the experimental data. This difference is mainly associated with the difference between the final state interactions for ^{4}He and ^{6}He [4,17]. On the other hand, the DWF parameter R is directly proportional to the rms radius of the nucleus in the final state [12,22], and we improved the DWTA calculation by changing R, obtained for ^{4}He, to

$$R' = R\,\frac{\sqrt{(R^n_{^6\mathrm{He}})^2 + (R_p)^2}}{R^{ch}_{^4\mathrm{He}}}, \tag{2}$$

where $R^{ch}_{^4\mathrm{He}} = 1.67(1)$ fm is the finite-nucleon rms radius of the charge distribution of ^{4}He [23], R_p is the proton charge radius (0.8 fm), representing the finite size of the nucleons, and $R^n_{^6\mathrm{He}}$ is a parameter to be fitted, the point-nucleon rms radius of ^{6}He. We also calculated the DWTA cross sections, using for $R^n_{^6\mathrm{He}}$ values taken from Refs. [1–4,10] (see below).

The residual nucleus of the reaction under study, ^{6}He, has a thick neutron cloud on the surface, or halo, so that $R^{ch}_{^6\mathrm{He}} \ll R^{n*}_{^6\mathrm{He}}$ [1–3], where $R^{n*}_{^6\mathrm{He}}$ is the finite-nucleon rms neutron distribution radius of ^{6}He. The energies of the protons interacting in the final state lay in the range 12–42 MeV and the wavelength, even for 42 MeV protons, is 5.2 fm, larger than the ^{6}He radius. So the final state interaction should be sensitive only to the surface properties of the residual nucleus: to $R^{n*}_{^6\mathrm{He}}$, but not to $R^{ch}_{^6\mathrm{He}}$.

Following this logic (see also [11]) we calculated, for the aim of comparison, the DWTA cross sections for the reaction ^{7}Li$(p,2p)^6$He, using the available experimental [1–4] and theoretical [10] values for $R^n_{^6\mathrm{He}}$. The results of such calculations are shown in Figs. 1 and 2, together with the result of the fitting $R^n_{^6\mathrm{He}} = 2.85(7)$ fm. This value agrees, within the uncertainties, with the result of Ref. [10]. The uncertainties presented ($\pm 3\%$) come from statistical and systematic uncertainties of our experimental cross sections, of experimental data used for the parametrization of the DWF, and from uncertainties in the radius of ^{4}He [23] as well. The high accuracy attained in the result for the ^{6}He radius arises from the high sensitivity of the calculated cross section to the radius of the residual nucleus. The result for the ^{6}He radius is model dependent in principle, because of the existence of some systematic errors associated with the models used to describe the reaction mechanisms and the FSI. Standard DWTA calculations for the cases ^{4}He-^{3}He, and ^{6}Li-^{7}Li, where experimental data for the radii are available, indicate that these systematic uncertainties are of a few percent. A direct estimate of these uncertainties, however, could be made only from the comparison with results obtained by different methods.

One may also notice from Figs. 1 and 2, that in the energy range under study, the quasifree cross sections are very sensitive to the $R^n_{^6\mathrm{He}}$ value. Changing the radius we are able to simultaneously fit calculations to the three data groups. For each group we used the DWF parameters for the average energy in the DWTA calculation. This simplification makes the curves in Figs. 1 and 2 discontinuous, although the errors introduced by this procedure are smaller than the experimen-

TABLE II. Parameters of the DWF for the exit channel (^{4}He) used in the DWTA calculation.

Proton energy (MeV)	β	γ	$\lvert F\rvert$	Arg(F) (degrees)	R (fm)	S (fm)
40	1.645	0.0094	3.4	130	1.683	3.00
31	1.645	0.014	3.4	130	1.780	3.00
22	1.645	0.029	3.4	130	2.087	3.00
14	1.922	0.485	8.0	130	2.14	3.00

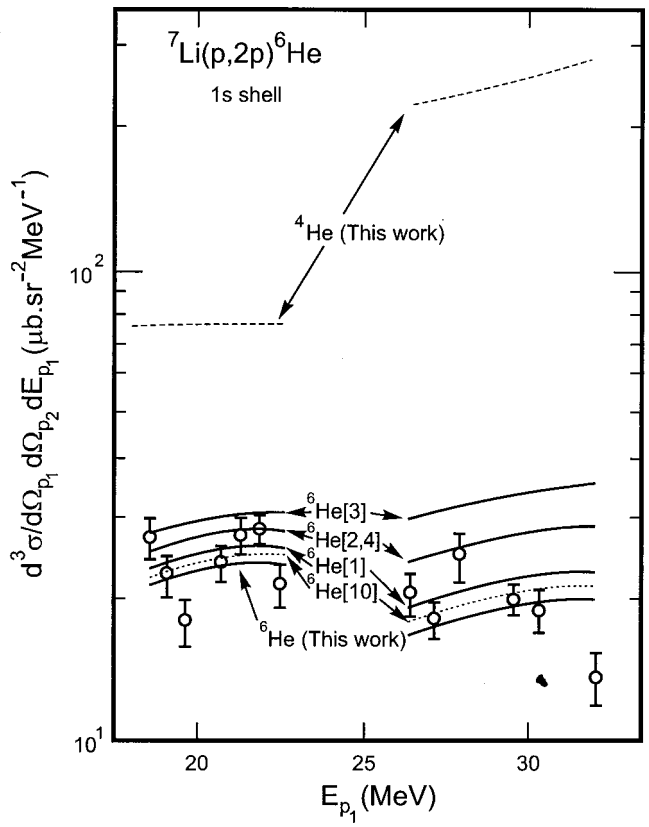

FIG. 1. Differential cross section for the reaction ^{7}Li(p,2p)^{6}He at $E_o = 70$ MeV, for the 1s shell. The curves represent results of the DWTA calculation (see text for details).

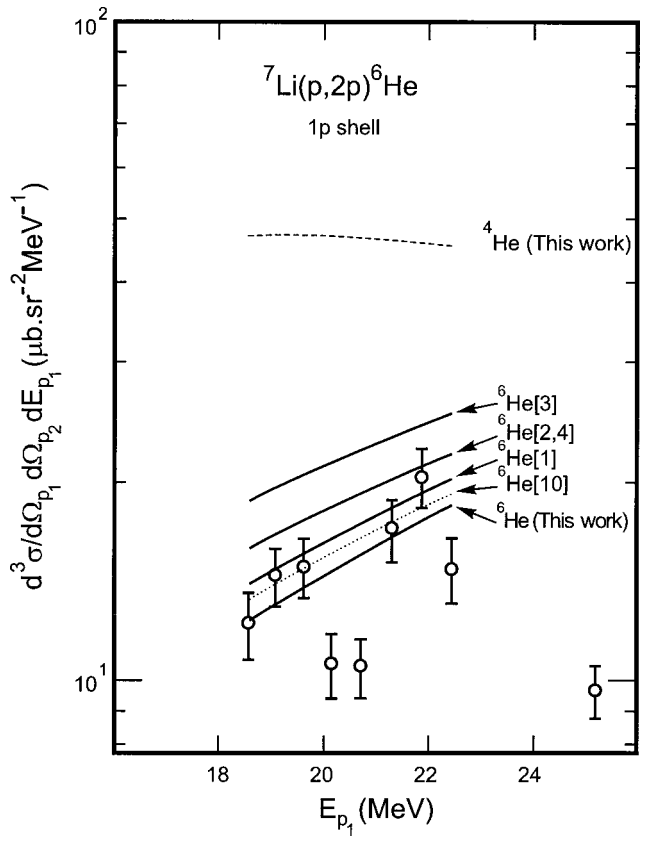

FIG. 2. Differential cross section for the reaction ^{7}Li(p,2p)^{6}He at $E_o = 70$ MeV, for the 1p shell. The curves represent results of the DWTA calculation (see text for details).

tal uncertainties, even close to the limits of the intervals. Note also that in the calculations the contribution of the nondirect knockout was taken into account [24]. This contribution is important since it is comparable with the difference between various previsions.

The DWTA calculations give a quantitatively correct description of the differential cross section for the reaction ^{7}Li(p,2p)^{6}He at $E_o = 70$ MeV, for both 1s and 1p shells, if the point-nucleon root-mean-square radius of the neutron distribution for ^{6}He is supposed to be 2.85(7) fm.

The cross section of the reaction ^{7}Li(p,2p)^{6}He at 70 MeV is sensitive to the radius of the residual nucleus, and if more accurate data become available, then the DWTA analysis may allow one to distinguish between the predictions of various models.

[1] I. Tanihata, H. Hashimoto, Y. Shida, N. Yoshikawa, K. Sugimoto, O. Yamakawa, T. Kobayashi, and N. Takahashi, Phys. Rev. Lett. **55**, 2676 (1985).
[2] I. Tanihata, T. Kobayashi, O. Yamakawa, S. Shimomura, K. Ekuni, K. Sugimoto, N. Takahashi, T. Shimoda, and H. Sato, Phys. Lett. B **206**, 592 (1988).
[3] G. D. Alkhazov *et al.*, Phys. Rev. Lett. **78**, 2313 (1997).
[4] I. Tanihata, D. Hirata, T. Kobayashi, S. Shimomura, K. Sugimoto, and H. Toki, Phys. Lett. B **289**, 261 (1992).
[5] J. S. Al-Khalili and J. A. Tostevin, Phys. Rev. C **57**, 1846 (1998).
[6] J. S. Al-Khalili *et al.*, Phys. Rev. C **54**, 1843 (1996).
[7] L. V. Chulkov *et al.*, Europhys. Lett. **8**, 245 (1989).
[8] K. Varda, Y. Suzuki, and Y. Ohbayasi, Phys. Rev. C **50**, 189 (1994).
[9] A. Csoto, Phys. Rev. C **48**, 165 (1993).
[10] K. Arai, Y. Suzuki, and K. Varda, Phys. Rev. C **51**, 2488 (1995).
[11] V. B. Shostak, G. P. Palkin, N. I. Woloshin, V. P. Likhachev, M. N. Martins, and J. D. T. Arruda-Neto, Phys. Rev. C **61**, 024601 (2000).
[12] P. C. Wright, R. G. Storer, and I. E. McCarthy, Phys. Rev. C **17**, 473 (1978).
[13] R. T. Janus and I. E. McCarthy, Phys. Rev. C **10**, 1041 (1974).
[14] M. I. Voloshin and A. D. Fursa, Ukr. Fiz. Zh. **39**, 1036 (1994).
[15] M. I. Voloshin and A. D. Fursa, Ukr. Fiz. Zh. **40**, 1171 (1995).
[16] M. V. Pasechnik *et al.*, Yad. Fiz. **54**, 616 (1991) [Sov. J. Nucl. Phys. **54**, 373 (1991)].
[17] V. B. Shostak, G. P. Palkin, N. I. Woloshin, V. P. Likhachev, J. D. T. Arruda-Neto, M. T. F. da Cruz, and M. N. Martins, Nucl. Phys. **A643**, 3 (1998).
[18] A. I. Vdovin, A. B. Golovin, and I. I. Loshchakov, Yad. Fiz.

42, 134 (1985) [Sov. J. Nucl. Phys. **42**, 84 (1985)].

[19] T. Y. Li and S. K. Mark, Can. J. Phys. **46**, 2645 (1968); R. F. Carlson *et al.*, Nucl. Phys. **A445**, 57 (1985); G. S. Moni *et al.*, *ibid.* **A165**, 145 (1971).

[20] D. J. Hugher and R. B. Schwartz, Neutron Cross Sections, Brookhaven National Laboratory, Upton, New York, 1958.

[21] V. S. Barashenkov and V. D. Toneev, *Interaction of High Energy Particles and Nuclei with Nuclei* (Atomizdat, Moscow, 1972).

[22] A. D. Bocher, G. R. Plattner, H. E. Conzett, D. J. Clark, H. Grunder, and W. F. Tivol, Phys. Rev. C **5**, 1147 (1972); N. K. Brussel and J. H. Williams, Phys. Rev. **106**, 286 (1957); D. Garreta, L. Sura, and A. Tarrats, Nucl. Phys. **A132**, 204 (1969); G. E. Thompson, M. B. Epstein, and T. Sawada, *ibid.* **A142**, 571 (1970); S. M. Bunch, H. H. Forster, and C. Clim, Nucl. Phys. **53**, 241 (1964).

[23] R. C. Barrett and D. F. Jackson, *Nuclear Sizes and Structure* (Clarendon, Oxford, 1977), p. 146.

[24] Y. Ikebata and Y. Kudo, Prog. Theor. Phys. **70**, 1457 (1983).